OFFICE OF NAVAL RESEARCH

Grant N00014-91-J-1274

R&T Code 413m005---04

Technical Report # UMR-FDB-22

Molecular Motions of the Head Group of SHBS in Lamellar Liquid Crystals

by

Joesph R. Duke, Robert B. Funchess and Frank D. Blum

Department of Chemistry and Materials Research Center
University of Missouri-Rolla
Rolla, MO 65401

(314) 341-4451

Prepared for Publication in

Langmuir

November 15, 1991

Abstract

Deuterium NMR spectra of a specifically-deuterated double-tailed surfactant sodium 4-(1'-heptylnonyl)benzenesulfonate (SHBS) both dry and in liquid crystals formed with water were obtained from -70 to 90 °C. The liquid crystalline deuterium powder patterns from the phenyl-ring deuterons can be described as from motions characterized as rigid (from -70 to -30 °C), two-fold ring flips (from -40 to -30 °C), and rotations in an anisotropic media (-20 °C and higher). For the higher temperature spectra (> -20 °C), the inclusion of a single fast rotation, or even anisotropic diffusion alone did not give the best fits of the experimental spectra. The inclusion of a local ordering potential, or anisotropic viscosity, yielded good fits to the experimental spectra. The local ordering potential required local order parameters from 0.856 to 0.763 for temperatures from 10 to 90 °C. The dry surfactant, in contrast to the liquid crystals at the same temperatures, undergoes both fast and slow two-fold ring flips at 25 °C with the fraction of fast flippers increasing with temperature.

Unclassified
SECURITY CLASSIFICATION OF THIS PAGE

REPORT DOCUMENTATION PAGE

1a. REPORT SECURITY CLASSIFICATION Unclassified	1b. RESTRICTIVE MARKINGS
2a. SECURITY CLASSIFICATION AUTHORITY	3. DISTRIBUTION / AVAILABILITY OF REPORT Approved for Unlimited Public Release
2b. DECLASSIFICATION / DOWNGRADING SCHEDULE	
4. PERFORMING ORGANIZATION REPORT NUMBER(S) UMR-FDB-22	5. MONITORING ORGANIZATION REPORT NUMBER(S)
6a. NAME OF PERFORMING ORGANIZATION University of Missouri-Rolla 6b. OFFICE SYMBOL (If applicable)	7a. NAME OF MONITORING ORGANIZATION Office of Naval Research (ONR)
6c. ADDRESS (City, State, and ZIP Code) Department of Chemistry University of Missouri-Rolla Rolla, MO 65401	7b. ADDRESS (City, State, and ZIP Code) Chemistry Division 800 Quincy Street Arlington, VA 22217-5000
8a. NAME OF FUNDING / SPONSORING ORGANIZATION 8b. OFFICE SYMBOL (If applicable)	9. PROCUREMENT INSTRUMENT IDENTIFICATION NUMBER N00014-91-J-1274
8c. ADDRESS (City, State, and ZIP Code)	10. SOURCE OF FUNDING NUMBERS PROGRAM ELEMENT NO. N00014-91 / PROJECT NO. J-1274 / TASK NO. / WORK UNIT ACCESSION NO

11. TITLE (Include Security Classification)

Molecular Motions of the Head Group of SHBS in Lamellar Liquid Crystals.

12. PERSONAL AUTHOR(S)
Joseph R. Duke, Robert B. Funchess, Frank D. Blum

13a. TYPE OF REPORT	13b. TIME COVERED	14. DATE OF REPORT (Year, Month, Day)	15. PAGE COUNT
Interum	FROM 1/90 TO 11/91	November 15, 1991	29

16. SUPPLEMENTARY NOTATION

For Publication in Langmuir.

17. COSATI CODES			18. SUBJECT TERMS (Continue on reverse if necessary and identify by block number)
FIELD	GROUP	SUB-GROUP	deuterium NMR spectroscopy, surfactants, liquid crystals.

19. ABSTRACT (Continue on reverse if necessary and identify by block number)

Deuterium NMR spectra of a specifically-deuterated double-tailed surfactant sodium 4-(1'-heptylnonyl)benzenesulfonate (SHBS) both dry and in liquid crystals formed with water were obtained from -70 to 90 °C. The liquid crystalline deuterium powder patterns from the phenyl-ring deuterons can be described as from motions characterized as rigid (from -70 to -30 °C), two-fold ring flips (from -40 to -30 °C), and rotations in an anisotropic media (-20 °C and higher). For the higher temperature spectra (> -20 °C), the inclusion of a single fast rotation, or even anisotropic diffusion alone did not give the best fits of the experimental spectra. The inclusion of a local ordering potential, or anisotropic viscosity, yielded good fits to the experimental spectra. The local ordering potential required local order parameters from 0.856 to 0.763 for temperatures from 10 to 90 °C. The dry surfactant, in contrast to the liquid crystals at the same temperatures, undergoes both fast and slow two-fold ring flips at 25 °C with the fraction of fast flippers increasing with temperature.

20. DISTRIBUTION / AVAILABILITY OF ABSTRACT ☒ UNCLASSIFIED/UNLIMITED ☒ SAME AS RPT ☐ DTIC USERS	21. ABSTRACT SECURITY CLASSIFICATION Unclassified
22a. NAME OF RESPONSIBLE INDIVIDUAL Kenneth J. Wynne	22b. TELEPHONE (Include Area Code) 703-696-4409 / 22c. OFFICE SYMBOL ONR (Chemistry)

DD FORM 1473, 84 MAR — 83 APR edition may be used until exhausted. All other editions are obsolete.

SECURITY CLASSIFICATION OF THIS PAGE
UNCLASSIFIED

Introduction

Sodium 4-(1'-heptylnonyl)benzenesulfonate (SHBS) is a double-tailed surfactant that has properties similar to many molecules of synthetic or biological origin. The surfactant shows no critical micelle concentration in water. It does show some evidence of aggregation below its solubility limit. With the further addition of surfactant, liquid crystals form which coexist with the soluble surfactant (1-3). Aqueous dispersions of these liquid crystals may be sonicated to form vesicles (4-7) and mechanically agitated to form liposome type structures (8). The structure of this surfactant is simpler than biological surfactants and its chemical and biological stability make it suitable for longer-term studies, at higher temperature.

Previous studies of the liquid crystals formed from SHBS and water have concentrated on the behavior of the water in the bilayers as well as the temperature dependence of the motions that the various segments of the surfactant undergo. These studies have identified a motional gradient within the hydrocarbon tails (9). The more restricted motion is toward the head group. The anisotropic behavior of the water associated with the head groups was also noted (8,10).

In order to investigate the motion of the head group, we have replaced the phenyl protons of SHBS with deuterons. The phenyl group is then the "labeled" site and used as a reporter group for the head group. The structure of the molecule is shown below.

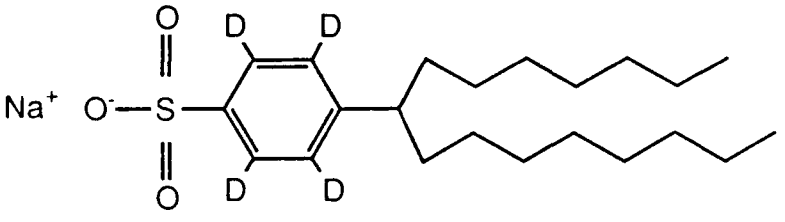

Sodium 4-(1'-heptylnonyl)benzenesulfonate

There are many factors which enable us to observe the motion of the phenyl group alone using deuterium NMR and several reviews exist (11-15). Due to deuterium's low natural abundance, an enriched species will be the dominant, if not the only, species observed with deuterium NMR spectrum. Deuterium spectra and relaxation rates for C-D species are dominated by the quadrupolar interaction which are related to the reorientation of a C-D bond vector. Both the rates and types of motion can be determined in favorable cases. Because of the magnitude of the quadrupolar interaction, it is possible to investigate motions with correlation times ranging over many orders of magnitude (13).

The deuterium nucleus has an electric quadrupole moment (spin I=1) and the nuclear transitions between spin states are perturbed slightly by an electric field gradient at the nucleus. The bond vector usually lies along one of the principal axes of the electric field gradient tensor (EFG). The magnitude of the perturbation is dependent upon the angle that the principal axis of the EFG makes with the magnetic field at the nucleus. Molecular motions produce spatial fluctuations of the EFG which alter the energies of the nuclear spin states. In the absence of molecular motion, two transitions would be observed for a singly labelled molecule with a given orientation. These correspond to transitions between z projections of spin angular momentum quantum numbers of $-1 \leftrightarrow 0$ and $0 \leftrightarrow 1$. For randomly oriented samples, a powder pattern spectrum is observed (11-15) which is due to the superposition of the two resonances for each of all possible molecular orientations. When molecular motion is present, there is a time averaging of this quadrupolar perturbation. By considering the rates and angles of the motion involved, it is possible to calculate the effect that motion will have on these two transitions. For example, for a set of deuterons with equivalent orientations, the difference in frequency ($\Delta\nu$) (in Hz) between the two transitions is given by :

$$\Delta\nu = \frac{3e^2qQ}{2h}\left\langle \frac{(3\cos^2\theta - 1)}{2} + \frac{\eta}{2}\sin^2\theta\cos 2\phi \right\rangle \quad (1)$$

where e^2qQ/h is the quadrupole coupling constant, θ is the angle that the C-D bond vector makes with the magnetic field, ϕ is the azimuthal angle, η is the asymmetry parameter, and the term in the <> will be time averaged over possible molecular orientations. The asymmetry parameter is usually small for C-D bonds.

In general, calculating a deuterium NMR spectrum requires considering all possible orientations that a C-D bond may have as well as the molecular motion it may undergo. When the effects of motion are considered, the spectra, normally some type of powder pattern, have shapes that are characteristic of both the type and rate of the motion that the molecules undergo. In the case of a phenyl group undergoing uniaxial reorientation, it is possible to distinguish between a molecule that is rigid, one undergoing fast ring flips, or one undergoing fast rotational diffusion as shown by Gall *et al.* (16) and later by Choli *et al.* (17). This is shown in Figure 1 as simulated with our program (18) for comparison with later spectra. For the static case, a Pake pattern with a quadrupolar splitting between the "horns" of 3/4 (e^2qQ/h) is expected. For fast 180° jumps, the splitting between the horns is reduced to 1/4 that of the static spectra and the overall shape changed as well. For fast free rotational diffusion about the symmetry axis, the spectral shape is similar to the static spectra, but the quadrupolar splitting is reduced to only 1/8 that of the static spectra (16,17).

A number of approaches for calculating deuterium line shapes and relaxation rates for postulated motional models currently exist and have been successfully applied to a variety of systems (19-28). Of these we have preferred to use the model from the work of Freed *et al.* (20,21) which is based on the

application of the stochastic Liouville equation for rotational motion. This program allows the simulation of spectra based upon jumps, free or Brownian diffusion, and inclusion of anisotropic viscosity effects. It has been modified by us for deuterium NMR (18).

In this paper we report the use of spectral lineshape analysis to determine the motion of the head group of the SHBS-d_4 (phenyl labelled) molecule both in the dry and liquid crystalline state. SHBS liquid crystalline powder samples are unoriented and contain many domains which have random orientations with respect to the magnetic field. Within each domain the molecules experience torques caused by mutual interactions with the other molecules. These interactions produce a longer range order which can be described by a restoring potential. These systems are microscopically ordered and macroscopically disordered. The director axis of a given liquid crystallite (Figure 2) determines the direction of the restoring potential. The model that describes time dependence of molecular reorientation, when described with respect to a space fixed axis, is termed anisotropic viscosity (29).

There have been a variety of other studies which gave used labelled phenyl rings for studying dynamics. In some small molecule solids, such as phenylalanine (16,30) the phenyl rings undergo two-fold ring flips, while in others the aromatic ring is rigid over a wide temperature range, as in nitroanaline (31). In biopolymer systems, ring flips occur in a number of systems (16,32,33). For highly crossed-linked synthetic polymer systems such as phenol-formaldehyde resins, the rings are rigid (34). When incorporated in the backbone of synthetic glassy bulk polymers or blends, the rings are generally characterized by rigid material plus material which undergoes ring flips (35-37). The ring flipping is often found superimposed on low amplitude torsional motions. These motions may also be altered by the presence of a diluent (38). In contrast, liquid crystalline

materials show increased local (and possibly macroscopic) order and also increased mobility. In these systems, the phenyl ring motions are often dominated by relatively fast motions about the symmetry axis (39-42).

Experimental

The surfactant SHBS was prepared according to the procedure given by Doe *et al.* (43). The starting material, an alkylphenylketone, was prepared by a Friedel-Crafts acylation of deuterobenzene with octanoyl chloride. Two samples were prepared for observation. A dry surfactant sample was prepared by drying the SHBS in a vacuum oven for 24 hours at 50 °C then adding the surfactant to a 5 mm NMR tube and sealing it. The liquid crystalline sample was prepared by adding the dry surfactant and deuterium depleted water to a 5 mm NMR tube and then sealing. The sample was then allowed to stand at room temperature for over a week until deuterium spectra showed only a single powder pattern. A slight excess of water was added to the surfactant to insure that all the surfactant present in the tube was hydrated. The surfactant soluble in the excess water was not deemed significant due to the limited solubility of SHBS in water and the small amount of excess water present. The composition of the liquid crystalline sample was 26 wt% water and 74 wt% SHBS.

The deuterium spectra were recorded on a Varian VXR-200 spectrometer operating with a wide line probe at 30.7 MHz for deuterium. Spectra were recorded using the solid echo pulse sequence (44):

$$(\pi/2)_x - \tau - (\pi/2)_y - \tau - \text{acquire}$$

with the $\pi/2$ pulse width adjusted to 2 μs. The delay between pulses, τ, was kept at 40 μs. Spectra below -10 °C were taken with a sweep width of 2×10^6 Hz, 16,000 points, 2,000 transients and line broadening of 2,000 Hz. In spectra at and above this temperature, the sweep width was changed to 2×10^5 Hz and the line broadening was changed to 200 Hz.

The sample was placed in the probe at room temperature and then the probe

was cooled to -70 °C; the cooling took less than 1 minute. The sample was allowed to stand at -70 °C for 10 min before spectra were recorded. The temperature was raised in 10° increments for each set of experiments ranging from -70 to 90 °C allowing 10 min at each temperature before spectra were again taken. After the initial 10 min wait, spectra were not observed to change even if left in the probe for several hours at any of the temperatures used in this study.

An ESR slow motional lineshape simulation program was modified for use with deuterium NMR (18). The program uses the slow motional theory developed by Freed to calculate theoretical lineshapes (20,21). We have used the options provided in the program that describe free rotational diffusion, jump diffusion, and anisotropic viscosity. All spectra simulated with the program use a quadrupolar coupling constant of 172 MHz determined from the quadrupolar splitting at -70 °C. Spectra simulated using the free and jump diffusion used an asymmetry parameter ($\eta = 0.04$) similar to that for other aromatic deuterons such as toluene, nitrobenzene, and benzene (45). Since the majority of the simulated spectra are for comparison with non-rigid spectra with splittings less than 20 kHz, no correction for pulse fall off was made.

For free diffusion, there are two rotational diffusion rates in Hz that describe the overall motion of the phenyl group. One rotational diffusion constant describes the rotation about the 1'-4' axis of the phenyl group (dzz), while a second rotational diffusion constant describes the rotation perpendicular to the long axis of the molecule (dxy) as shown in Figure 2. In addition, specification of the diffusion tilt angle is needed. This is the angle between the 1'-4' phenyl diffusion axis and the magnetic frame, *i.e.* the C-D bond vector. This angle is taken to be 60° for this case.

For jump-type motions, additional parameters are needed to describe the jump. These parameters include the diffusional jump frequency and the number of equivalent sites (in this case 2). The axis of the jump-type motion is taken to be

parallel to the 1'-4' axis of the phenyl group as shown in Figure 2.

The spectra simulated using the anisotropic viscosity model are composite spectra. Ninety spectra were calculated for director orientations (β') ranging from 1° to 90° with respect to the magnetic field. The resulting spectra were then normalized, weighted, and added together. The weighting applied to each spectrum was sin β' which is representative of an isotropic distribution of angles. Several parameters are used in addition to the director orientation β' in the calculation of individual spectra. These include two rotational diffusion rates (dzz and dxy), the diffusion tilt angle, and a restoring potential. In this model, dzz refers to motion about the director axis and dxy refers to motions that change the angle between the molecular symmetry axis (the 1'-4' axis) and the director axis. The diffusion tilt angle was taken to be 60°. The restoring potential is responsible for reorienting the molecules along the director axis. In order to derive a restoring potential we have used the experimental quadrupolar splitting. The quadrupolar splitting can be related to the equilibrium orientational average of the Wigner rotation matrix element $\langle D^2_{00} \rangle$ which relates tensor components in the molecular fixed frame to those in the director fixed frame. Assuming a fast rotation about the 1'-4' axis, the quadrupolar splitting for a single ring deuteron is given by (39):

$$\Delta\nu = \frac{3e^2qQ}{2h} P_2(\cos\beta') P_2(\cos\beta'') \langle P_2(\cos\beta) \rangle \qquad (2)$$

where, β is the angle between the molecular symmetry axis and the director, β' is the angle between the director and the magnetic field, and β'' is the angle between the C-D bond vector and the molecular symmetry axis, and terms like $P_2(\cos\alpha)$ are given by :

$$P_2(\cos\alpha) = \left(3\cos^2\alpha - 1\right)/2 \qquad (3)$$

In this notation $<P_2(\cos\beta)>$ is the local order parameter and the angular brackets denote a time averaging. The local order parameter can be related to the restoring potential through the following equation (20):

$$\left\langle D^2_{00}\right\rangle = \left\langle P_2(\cos\beta)\right\rangle = \frac{\int P_2(\cos\beta)\exp\left[-U(\beta)/kT\right]\sin\beta\, d\beta}{\int d\beta\, \exp\left[-U(\beta)/kT\right]\sin\beta\, d\beta} \qquad (4)$$

The form of the restoring potential used in the calculation is given by $-U(\Omega)/kT = \lambda^2 P_2(\cos\beta)$. Trial values of λ were chosen and equation (4) was solved until the calculated order parameter converged to the experimental order parameter, as determined by $\Delta(90°)$ from the experimental spectrum. The experimental order parameter was calculated from equation (3) for $\beta' = 90°$ and $\beta'' = 60°$.

Results

The experimental deuterium NMR spectra obtained at and below -20 °C are shown in Figure 3. The spectra from -70 °C to -50 °C are typical Pake patterns corresponding to molecules undergoing motions much slower than the breadth of the powder pattern (*i.e.* slower than 260 kHz). The two peaks in these spectra correspond to the direction of the C-D bond vector being oriented at 90° with respect to the magnetic field. The quadrupole splitting, $\Delta(90°)$, is defined as the frequency (in Hz) between these two horns. From -70 to -50 °C, $\Delta(90°)$ is approximately constant at 128 kHz. As the temperature is increased to -40 °C, an inner powder pattern with a $\Delta(90°)$ of 33 kHz emerges plus a small central resonance. The 33 kHz powder pattern is relatively more intense at -30 °C. The quadrupole splitting of the inner pattern at -20 °C is further reduced to 13.5 kHz. There is also an indication of another broad component in the baseline, but at this temperature the spectrum is mostly due to the species with the smaller splitting. The intensities of the spectra at -40 and -30 °C are reduced with respect to the intensities of spectra taken above and below this temperature. Motions with frequencies on the order of the spectral width cause this type of intensity reduction (46). The superposition of different motional species in these spectra made it difficult to do detailed lineshape analyses on these spectra.

From -20 to 90 °C, $\Delta(90°)$ decreases continually from approximately 14 kHz at -20 °C to 12.3 kHz at 90 °C but the lineshape remains relatively constant. The quadrupolar splittings for temperatures from 10 to 90 °C are given in Table 1. Figure 4 shows some of the spectra over this interval along with simulations (see below). Note that the intensity scale is highly expanded relative to Figure 3. At 50 °C, a second quadrupole splitting is observed, although hints of it seem to appear in the spectrum at 30 °C as well. The reason for this second splitting is not known, but it could be due to the presence of a second phase, with its own powder

pattern, in which the surfactant's motion differs somewhat from that in the lamellar phase. It could also be indicative of a small amount of oriented liquid crystal, although no evidence of this from D_2O in between the bilayers was observed (47).

The spectra of the dry surfactant, SHBS-d_4, taken at 25 and 90 °C are shown in Figure 5. The spectra show powder patterns plus a single central portion. The central feature may be due to a small amount of isotropic material as the solid is non-crystalline. The $\Delta(90°)$ decreases from 33 kHz at 25 °C to 28 kHz at 90 °C. The line shape is changed as well. At 25°C, the spectrum of the dry surfactant shows a broad component with shoulders at a separation of 125 kHz. The suppression of this broader pattern in the spectra (Figure 5C) of the dry surfactant was accomplished with a π pulse and a delay of 0.06 seconds preceding the quadrupole echo sequence.

Shown in Figure 6 are spectra in which we have modeled the two types of motions, free rotational diffusion and jump type diffusion. Spectra in Figure 6 from A to E correspond to free, but anisotropic, rotational diffusion. In spectrum A of Figure 6, $\Delta(90°)$ is 120 kHz. Our simulation requires the use of two non-zero rotational rates. Thus, we are not able to simulate a totally rigid spectrum. This small amount of motion accounts for the differences between 120 kHz simulated and 128 kHz expected. As the rotational diffusion rate about the 1'-4' axis is increased, the splitting between the two peaks decreases. The features broaden until at dxy = 1 MHz only one broad feature is observed. Further increases in the 1'-4' rotational diffusion rate causes the appearance of a powder pattern which is similar in shape to that of a rigid powder pattern, but with decreased quadrupole splitting, $\Delta(90°)$, of approximately 13 kHz.

The effects of jump motions with frequencies ranging from 100 kHz to 10 MHz is also shown in Figure 6F-H. Over this range of frequencies, the spectra are most affected by this jump-type motion. Splittings for $\Delta(90°)$ of approximately 30

kHz are found for fast jumps. Jump spectra simulated with a jump frequency greater than 10 MHz are similar in appearance to Figure 6H.

For the relatively fast free-diffusion case, expanded spectra are shown in Figure 7. These spectra are within the range of splittings shown in the experimental spectra of Figure 4 and are calculated assuming a constant dzz with a varying dxy. Increasing the rotational diffusion rate, dzz, from 10 MHz has no further effects on spectral line shape. There is a narrowing of the quadrupole splitting $\Delta(90°)$ from 13 kHz to 10 kHz as the rotational diffusion rate perpendicular to the long axis, dxy, changes from 900 Hz to 1700 Hz. As this rate of rotation increases further, the splitting narrows and eventually collapses to one peak (not shown). It is noted that the features of these spectra are not consistent with the experimental spectra, especially in the outer wings, even though the quadrupolar splittings $\Delta(90°)$ can be matched.

Spectra simulated using the anisotropic viscosity model are shown in Figure 4 along with the experimental spectra taken at 10°C and above. The rotational diffusion rates dxy and dzz are 1 MHz and 10 MHz, respectively, the value determining the ordering potential was varied, and a line broadening of 300 Hz was used. Spectra simulated with dzz less than 10 MHz are broadened, especially in the wings (outer edges) $\Delta(180°)$, and their shapes unlike the experimental spectra. Spectra simulated with dxy less than 1 MHz become more like the spectra simulated with the free diffusion simulated spectra. As both dxy and dzz become larger than 1 and 10 MHz, respectively, the spectral features become much sharper and are also different from the experimental ones. Spectra simulated with these faster rates can be made to fit those shown in Figure 4 by increasing the line broadening. Therefore the anisotropic viscosity lineshape provides us with a minimum rate of rotation for dxy and dzz.

Discussion

Previous studies on SHBS-water liquid crystals by ^{13}C NMR and DSC (9) indicated that at -70 °C, the hydrocarbon tails of surfactant melt, and that from -50 to -10 °C the bilayer water of these liquid crystals melts. That study also suggested a transition at -23 °C that corresponded to the melting of the water associated with the ionic part of the head group.

The deuterium NMR experiments of this study also show similar trends for the liquid crystal samples. The deuterium spectra for the head group below -40 °C are similar to rigid spectra. From -40 to -30 °C, there is an indication that some of the rings of the phenyl group begin to flip and that the fraction of fast flippers increases with temperature. The splitting of the spectrum is similar to that of Figure 1B (16). At -20 °C, the first indication of fast free rotational diffusion of the phenyl group is observed. In addition, may be just a slight amount of fast flipping rings are still present at this temperature. Similar jump like spectra have been seen in polymer systems in which the environment around the phenyl ring is restricted (35-37). In this case, the restriction responsible for allowing flipping may be the water frozen in between the bilayers. When the water unfreezes , the ring is allowed to spin freely, although, this is probably a cooperative event between the two species.

From -20 to 90 °C, the spectra from the head-group are indicative of a fast continuous rotation of the phenyl group about the long axis (dzz) of the molecule. The most significant changes are a decrease in the quadrupolar splitting and the appearance of a small amount of a second component with temperature. The splitting, however, is reduced from the 16 kHz expected from free rotation about the symmetry axis alone (Figure 1) (16). Inclusion of the rotation about the perpendicular axis of the phenyl ring into the model yields the spectra which fit the quadrupolar splitting, but do not fit the experimental spectra well. This is

especially obvious in the wings of the spectra where those of the simulated spectra (Figure 7) are broader than those of the experimental ones (Figure 4, left). Therefore, other factors must be responsible for the effects observed in the experimental spectra. The lineshapes of the spectra calculated using the anisotropic viscosity model are more like the experimental spectra over this temperature range. The fits are quite good, especially at lower temperatures. At higher temperatures, the "middle" of the experimental spectra are a bit more intense possibly because of the presence of the "other" horns in the spectrum. The lineshape simulations clearly show that the motion of the surfactant's head group is well described by rotational diffusion subject to a restoring potential. In addition, the local ordering in the liquid crystal plays a major role in the reduction of the splitting and lineshape rather than the rotational diffusion rates. Thus, in this case, the lineshapes provide significant insight into the local ordering in the bilayers.

There are also other modes of motion that could be alternative ways to understand spectra taken for liquid crystals. These could include other internal rotations (42), the collective fluctuations of molecules in the bilayer, and even the diffusion over a curved surface (48) or ribbon phase (49), across defects in the bilayer structure, and uniform diffusive wobbling in a cone (28). The latter can be used to gain information on the extent of the head groups restriction. In this model, the order parameter is related to the cone half angle, θ_0, by (28):

$$\left\langle D^2_{0\,0} \right\rangle = \frac{1}{2}\cos\theta_0\left(1+\cos\theta_0\right) \qquad (5)$$

Application of this model to our spectra based on $\left\langle D^2_{0\,0} \right\rangle$ or $\langle P_2 \rangle$, as obtained from equation 3, yields values from 0.851 at 10 °C to 0.758 at 90 °C as shown in Table 1. These correspond to a cone of half angle from 25.7° at 10 °C to 33.6° at 90 °C.

Information obtained from T_1 relaxation measurements of SHBS liquid crystals over this temperature range indicate one of the motions, dxy or dzz, is near the Larmor frequency of the deuterium nucleus (47). This is consistent with the rates obtained from our simulations.

The motion in the dry SHBS contrasts nicely with the liquid crystalline SHBS studied over the same temperature range. The motion of the dry surfactant is more restricted than that in the liquid crystal. At 25 °C, the dry surfactant appears to have an immobile component plus one which undergoes ring flips--whereas the liquid crystalline surfactant undergoes a fast continuous diffusive type motion at the same temperature. At 90 °C the most of the phenyl rings appear to be undergoing the flipping type motion. No evidence of fast continuous rotation is found for the dry surfactant.

Conclusions

The addition of water to dry SHBS significantly increases the mobility of the head group. The head group motion is still restricted with respect to reorientation away from the director axis. The surfactant's interaction with water and other surfactant molecules is such that the environment around the head group favors fast rotational reorientation of the phenyl ring about the 1'-4' axis at higher temperatures (> -20 °C). This motion is simulated by the inclusion of a fast reorientation about the symmetry axis, a slower motion perpendicular to it, and also the presence of a fairly strong local ordering potential. At lower temperatures (< -20 °C), 2-fold ring flips occur and are frozen out, on the NMR timescale, at lower temperatures (< -40 °C), after which a static powder pattern remains. In contrast, the dry surfactant shows evidence of static, ring flipping, and possibly even isotropic components at room temperature. At 90 °C, the ring flips and isotropic species dominate. The fast rotational reorientation, in the liquid crystals, contrasts sharply the phenyl ring motion in solids and polymer systems (16,17,34-38) where ring flips dominate. On the other hand, the behavior of the solid surfactant was similar to bulk polymers in terms of motional mechanisms (ring flips). Liquid crystalline systems with mobility greater than those in bulk polymers undergo fast rotation as well as demonstrated by relaxation behavior (39-42).

Finally, it should be noted that in addition to the two rotational rates used in the model, the local ordering dominates to large extent the spectral features. Thus, these experiments provide evidence of the local environment in terms of structure as well as dynamics.

Acknowledgements

The authors wish to thank H. S. Won for preparing the deuterated surfactant and the Office of Naval Research for their financial support of the project.

References

1. Miller, W. G.; Blum, F. D.; Davis, H. T.; Franses, E. I.; Kaler, E. W.; Kilpatrick, P. K.; Nietering, K. E.; Puig, J. E.; Scriven, L. E. Surfactants in Solution; Mittel, K. L.; Lindman, B. eds.; Plenum Publishing, New York, 1984; 1, pp. 175.
2. Franses, E. I.; Davis, H. T.; Miller, W. G.; Scriven, L. E. Chemistry of Oil Recovery; Johansen, R. T.; Berg, R. L. eds.; American Chemical Society, Washington, 1979, pp. 35.
3. Kilpatrick, P. K.; Miller, W. G. *J. Phys. Chem.* **1984**, *88*, 1649.
4. Kilpatrick, P. K.; Miller, W. G.; Talmon, Y. *J. Colloid Interface Sci.* **1985**, *107*, 146.
5. Franses, E. I.; Talmon, Y.; Scriven, L. E.; Davis, H. T.; Miller, W. G. *J. Colloid Interface Sci.* **1982**, *86*, 449.
6. Kaler, E. W.; Falls, A. H.; Davis, T. H.; Scriven, L. E.; Miller, W. G. *J. Colloid Interface Sci.* **1982**, *90*, 424.
7. Madani, H.; Kaler, E. W. *Langmuir* **1990**, *6*, 125.
8. Blum, F. D.; Franses, E. I.; Rose, K. D.; Bryant, R. G.; Miller, W. G. *Langmuir* **1987**, *3*, 448.
9. Blum, F. D.; Miller, W. G. *J. Phys. Chem.* **1982**, *86*, 1729.
10. Franses, E. I.; Miller, W. G. *J. Colloid Interface Science* **1984**, *101*, 500.
11. Seelig, J. *Quart. Rev. Biophys.* **1977**, *10*, 353.
12. Mantsch, H.; Saito, H.; Smith, I. P. *Prog. NMR Spectros.* **1977**, *11*, 211.
13. Bovey, F. A.; Jelinski, L. W. *J. Phys. Chem.* **1985**, *89*, 571.
14. Jelinski, L. W. in High Resolution NMR Spectroscopy of Synthetic Polymers in Bulk, Komoroski, R. ed.; VCH Publishers, 1986.
15. Davis, J. H. *Biochem. Biophys. Acta.* , **1983**, *737*, 117.
16. Gall, C. M.; DiVerdi, J. A.; Opella, S. J. *J. Am. Chem. Soc.*, 1981, *103*, 5039.
17. Cholli, A. L.; Dumais J. J.; Engle A. K.; Jelinski, L. W. *Macromolecules* **1984**, *17*, 2399.

18. Jagannathan, S.; Polnaszek, C.F.; Blum, F.D. *J. Chem. Inf. Comput. Sci.* **1987**, *27*, 167.
19. Alexander, S.; Baram, A.; Luz, Z. *Mol. Phys.* **1974**, *27*, 441.
20. Freed, J. H. Spin Labeling: Theory and Applications,Vol 1; Academic Press, Inc., New York, 1976.
21. Schneider, D. J.; Freed, J. H. Spin Labeling: Theory and Applications, Vol. 8; Academic Press, Inc., New York, 1989.
22. Meirovitch, E.; Freed, J.H. *Chem. Phys. Lett.* **1979**, *64*, 311.
23. Speiss, H. W. *in*.NMR, Basic Principles and Progress. Vol. 15, Diehl, P.; Fluck, E.;Kosfeld, R. eds.; Springer-Verlag, Berlin, 1978.
24. Torchia, D. A.; Szabo, A. *J. Magn. Reson.*, 1982, *49*, 107.
25. Mehring, M.; High Resolution NMR in Solids, Springer-Verlag, New York, 1983.
26. Muller, K.; Meier, P.; Kothe, G. *NMR Spectros* **1985**, *17*, 211.
27. Greenfield, M. S.; Ronemus, A. D.; Vold, R. L.; Vold, R. R. *J. Magn. Reson.* **1987**, *72*, 89.
28. Vold, R. R.; Vold R. L. Advances in Magnetic Resonance, Vol. 16; Academic Press, Inc., New York, 1991.
29. Polnaszek, C. F.; Bruno, G. V.; Freed, J. H. *J. Chem. Phys.* **1973**, *58*, 3185.
30. Frey, M. H.; DiVerdi, J. A.; Opella, S. J. *J. Am. Chem. Soc.*, **1985**,*107*,7311.
31. Kennedy, M. A.; Vold, R. R.; Vold, R. L. *J. Magn. Reson.* **1991**, *91,* 301.
32. Rice, D. M.;Wittebort, R. J.; Griffin, R. G.; Meirovitch, E.; Stimson, E. R.; Meinwald, Y. C.; Freed, J. H.; Scheraga, H. A. *J. Am. Chem. Soc.*, **1981**, *103*, 7707.
33. Meirovich, E. ; Samulski, A. L.; Scheraga, H. A.; Rananavare, S.; Nemethy, G.; Freed, J. H. *J. Phys. Chem.*, 1987, *91*, 4840.
34. Kelusky, E. C.; Fyfe, C. A.; McKinnon, M. S. *Macromolecules*, 1986, *19*, 329.
35. Smith, P. B.; Bubeck, R. A.; Bales, S. E. *Macromolecules* **1988**, *21*, 2058.

36. Henrichs, P. M.; Luss, H. R.; Scaringe, R. P. *Macromolecules*, 1989,*22*, 2731.

37. Dumais, J. J.; Jelinski, L. W.; Galvin, M. E.; Dybowski, C.; Brown, C. E.; Kovacic, P. *Macromolecules* **1989**, *22*, 612.

38. Smith, P. B.; Moll, D. J. *Macromolecules*, 1990, *23*, 3250.

39. Dong, R. Y. *Mol. Cryst. Liq. Cryst.* **1986**, *141*, 349.

40. Dong, R. Y.; Richards, G. M. *Chem. Phys. Lett.* **1990**, *171*, 389.

41. Beckman, P. A.; Emsley, J. W.; Luckhurst, G. R. *Molecular Physics*, **1986**, *59*, 97.

42. Vold, R. R.; Vold, R. L. *J. Chem. Phys.* **1988**, *88*, 1443.

43. Doe,P. H.; El-Emary, M., Wade, W. H.; Schechter, R. S. *J. Am. Oil Chem Soc.* **1977**, *54*, 570.

44. Davis, J. H.; Jeffery, K. R.; Bloom, M.; Valic, M. I.; Higgs, T. P. *Chem Phys Lett.* **1976**, *42*, 390.

45. Caniparoli, J.; Bredel, T.; Chachaty, C.; Maruani, J. *J.Phys. Chem.* **1989**, *93*, 797.

46. Speiss, H. W.; Sillescu, H. *J. Magn. Reson.* **1981**, *42*, 381.

47. Duke, J. R.; Blum, F. D. unpublished results.

48. Davis, J. H. *Biochemistry* **1988**, *27*, 428.

49. Chidichimo, G.; Vaz, N. A. P.; Yaniv, Z.; Doane, J. W. *Phys. Rev. Lett.* **1982**,*49*,1950.

Table 1: Experimental quadrupolar splittings, order parameters, and cone angles for SHBS head-group reorientation.

T (°C)	$\Delta\nu$ (kHz)	$\langle P_2(\cos\beta)\rangle$	θ_o
10	13.8	0.856	25.7
30	13.5	0.837	27.5
50	12.9	0.800	30.7
70	12.5	0.775	32.7
90	12.3	0.763	33.6

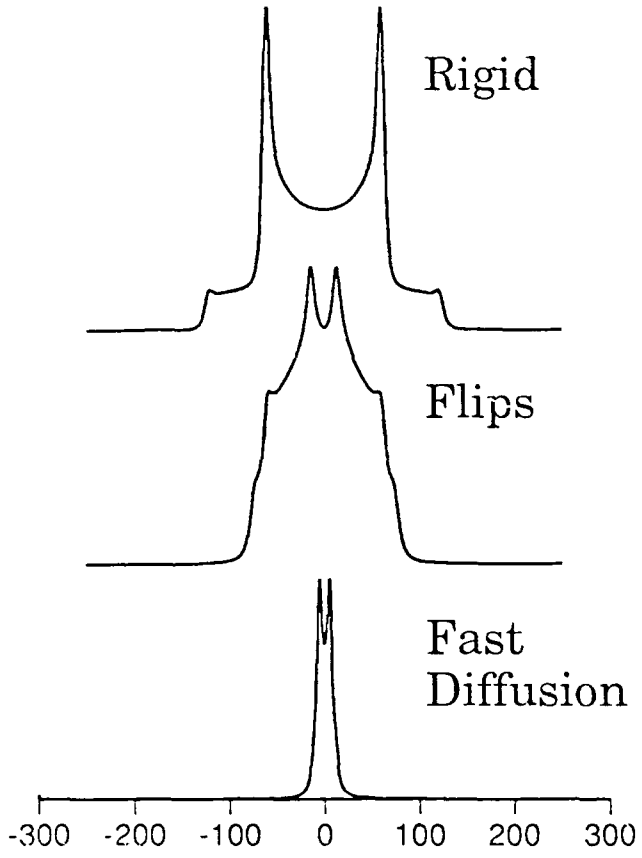

Figure 1. Deuterium NMR spectra for aromatic deuterons for rigid or static Pake pattern; ring flips; and fast uniaxial rotational diffusion (after references 16,17).

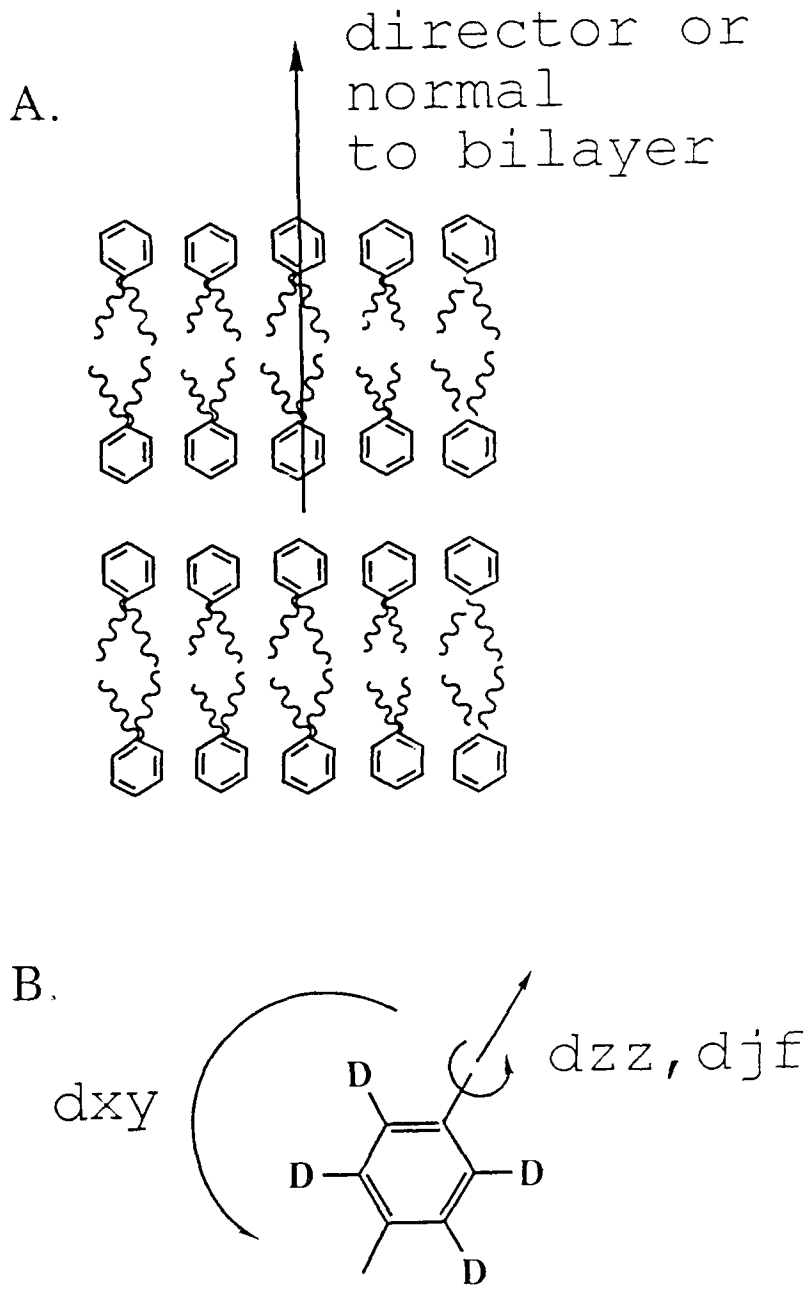

Figure 2. (A) Illustration of lamellar liquid crystal with the director axis of the bilayer. The sulfonate group is not shown. (B) Diagram of axis of rotation of phenyl head group. Parameters dxy, dzz,and djf are two rotational diffusion rates and the jump rate between sites, respectively.

FIG 2

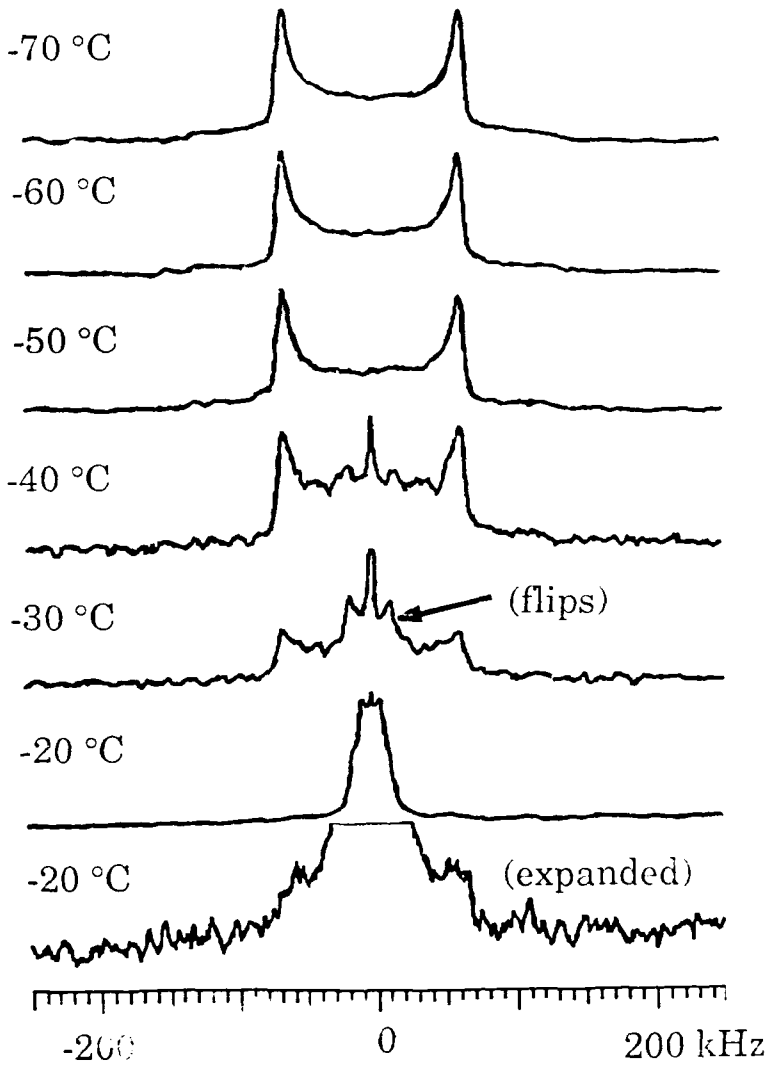

Figure 3. Experimental deuterium NMR spectra of SHBS liquid crystals from -70 to -20 °C. The intensity of the spectra at -20 °C has been increased in the bottom spectrum in order to see the broader features.

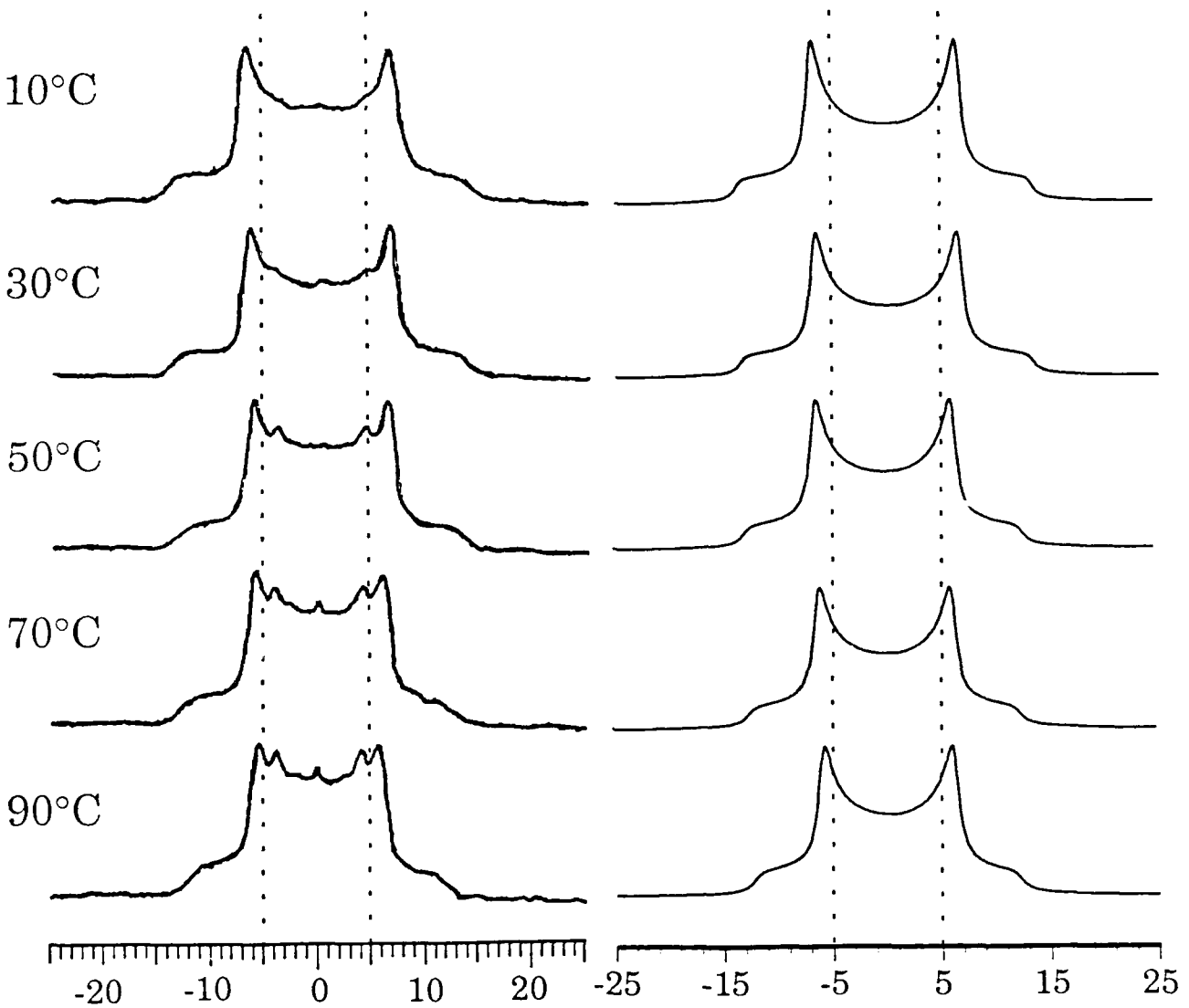

Figure 4. Experimental (left) deuterium NMR spectra of the liquid crystals of SHBS from 10 to 90 °C and corresponding simulations (right) using the model including anisotropic viscosity.

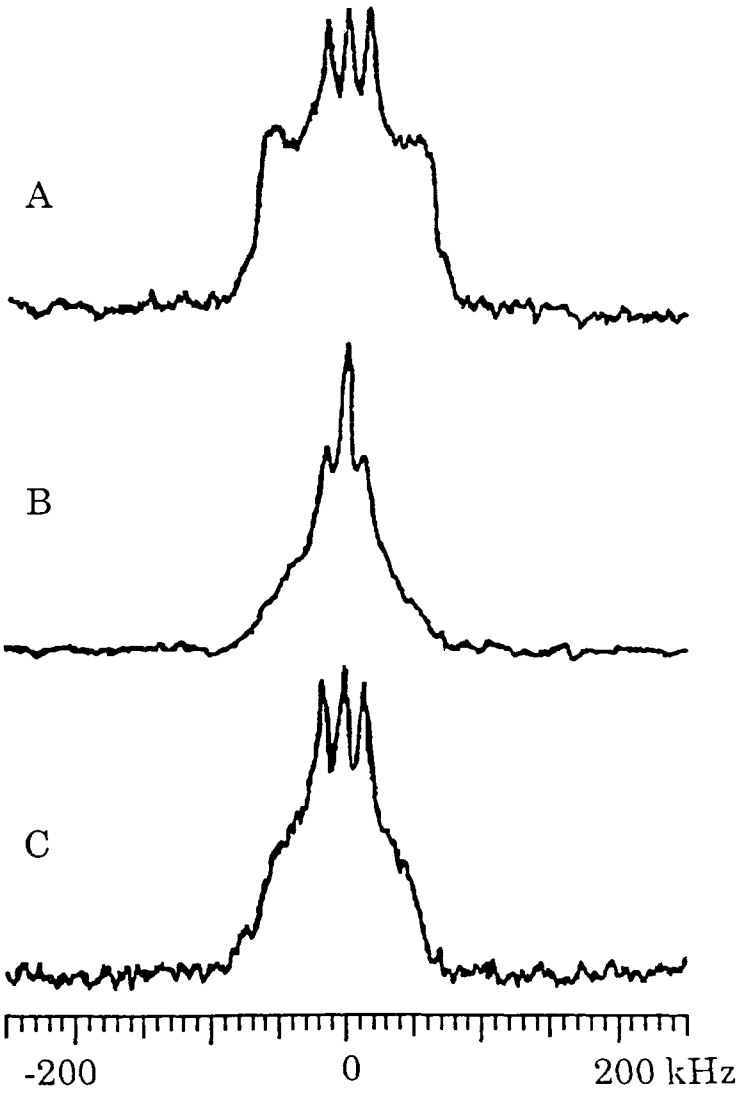

Figure 5. Experimental deuterium NMR spectra of dry SHBS (A) at 25 °C, (B) 90 °C, and at 25 °C where the broad pattern has been eliminated by an inversion pulse in (C).

FIG. 5

Figure 6. Calculated spectra from aromatic deuterons undergoing free rotational diffusion (left) and and jump diffusion (right). For free rotational diffusion, with dxy held constant at 10^3 Hz, dzz=: A) 10^3 Hz; B) 10^4 Hz; C) 10^5 Hz; D) 10^6 Hz; E) 10^7 Hz. For jump diffusion, a slow diffusive motion of dxy = dzz = 10^3 Hz, superimposed on the jump motion, djf=: F) 10^5 Hz; G) 10^6 Hz; H) 10^7 Hz was used.

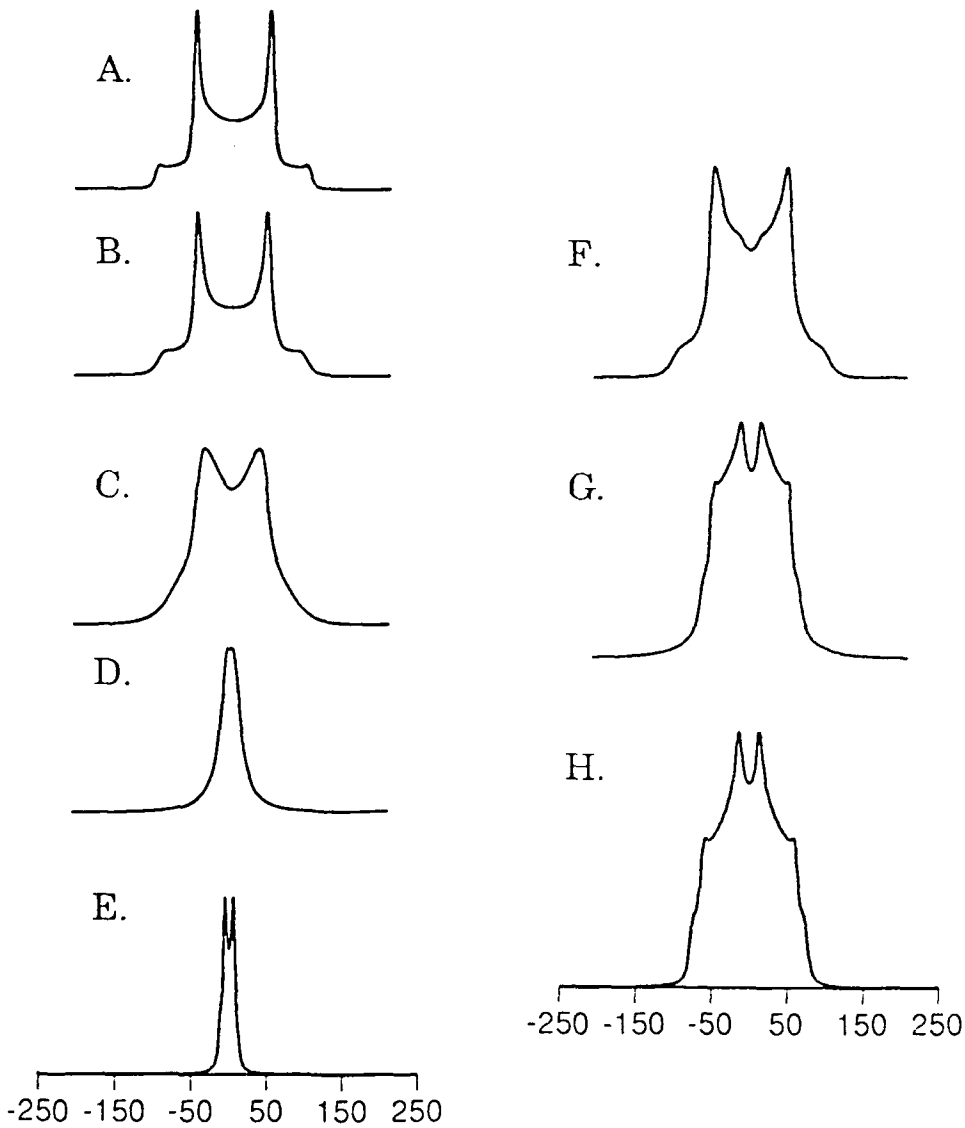

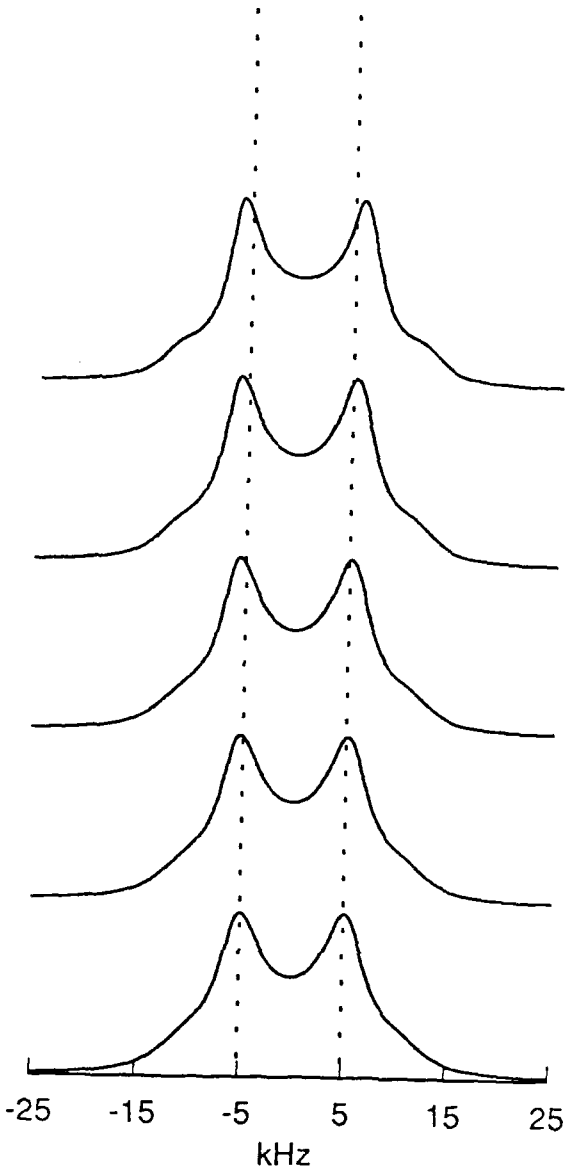

Figure 7. Calculated spectra of molecules undergoing free rotational diffusion; dzz is held constant at 10^7 Hz while dxy increases from 900 Hz (top) to 1700 Hz (bottom) in 200 Hz increments. The values are in the range of splittings which correspond to Figure 3.